Geothermal Resources Council, TRANSACTIONS, Vol. 12, October 1988

BEHAVIOR OF AN ARTIFICIAL RESERVOIR CREATED IN A FORMATION WITH A NATURAL FRACTURE NETWORK FOR HDR GEOTHERMAL HEAT EXTRACTION

Kazuo Hayashi(1) Kohei Kumazawa(2) and Hiroyuki Abé(3)

(1) Institute of High Speed Mechanics, Tohoku University, Sendai 980, Japan
(2) Recruit Co. Ltd., Chuo-ku Kachidoki 2-11, Tokyo 104, Japan
(3) Faculty of Engineering, Tohoku University, Sendai 980, Japan

ABSTRACT

Growth behavior of an artificially created reservoir system for HDR geothermal heat extraction in a formation with a natural fracture network, is analysed for the stage of the creation of the reservoir system by hydraulic fracturing and also for the stage of fluid circulation through the reservoir system. It is revealed that the reservoir system grows up with an elliptical shape and its growth rate rapidly decreases with time after the circulation of fluid through the reservoir system starts. The fluid loss during the circulation has been found to be fairly small and the most amount of the injected fluid can be recovered: more than 80% of the injected fluid, for example, can be recovered when the permeability of the natural fractures is less than $2 \times 10^{-10} m^2$. This implies that, even if a natural fracture network exists in a formation, it is possible to extract heat from such a formation by using an artificially created reservoir system.

INTRODUCTION

After the basic concept of the heat extraction from HDR was proposed (Smith et al., 1973), several HDR projects were begun in US, UK, Japan, France and West Germany. In the basic concepts, a large artificial crack and/or large artificial multiple cracks are considered to be subsurface heat exchange surfaces, and such subsurface systems for the geothermal heat extraction have actually been constructed in some cases. The typical example is the subsurface system of the Γ-project, Tohoku University (Takahashi and Abé, 1988). However, as well known, in the cases of the Geothermal Project of the Camborne School of Mines, UK (Garnish, 1985) and of Phase II of the HDR Project of Los Alamos National Laboratory, US (Whetten et al., 1987), the subsurface systems consist of large number of natural fractures.

In the course of these two Projects, numerical simulations of the subsurface reservoir systems have been performed (Murphy, 1982; Pine and Cundall, 1985) by using the computer program FRIP, which is based on the Distinct Element Method (Cundall, 1983) and was developed by Cundall (Murphy, 1982). However, the simulations are restricted to their own fields only and, as a results, the results of the simulations are specific to each field concerned. So far, there are very restricted knowledge on the behavior of the artificial subsurface reservoir systems created in strongly fractured rock masses.

In the present paper, we deal with a formation with natural fractures and analyze the interaction between the elastic deformation of the formation and the flow of fluid injected into the formation, to grasp the behavior of the reservoir system created artificially in a strongly fractured rock mass. The reservoir system consists of a main flow path of fluid and subsidiary flow paths which surround the main flow path. The main flow path is along one of the natural fractures which is subjected to a least compressive tectonic stress normal to it and, among the fractures, is most easily opened up by the pressure of injected fluid. The subsidiary flow paths are along the natural fractures which are neighboring with or intersecting the main flow path, and these natural fractures are presumably closed because of higher compressive tectonic stresses acting normal to them and/or the drop of fluid pressure due to flow resistance along them. The opened region of the main flow path is modeled as a crack along an interface with infinitesimally small fracture toughness.

It has been revealed that the shape of the reservoir system is elliptical, where its aspect ratio is almost conserved after it becomes fairly large, and its growth rate decreases with time after the circulation of fluid through the reservoir system starts. The fluid loss has been found to be fairly small during the circulation and most amount of injected fluid can be recovered.

INJECTION OF FLUID INTO A FORMATION WITH A FRACTURE NETWORK

Consider a formation with large natural fractures. The formation is contained between two intact formations (fig. 1). Suppose a hydraulic fracturing is performed in the naturally fractured formation, then the fracturing fluid flows along the natural fractures and a reservoir system consisting of many fluid flow paths along the natural fractures is created. For such a reservoir system, it is highly probable that, among the many fractures, only a specific fracture being subjected to a least compressive tectonic stress will be opened

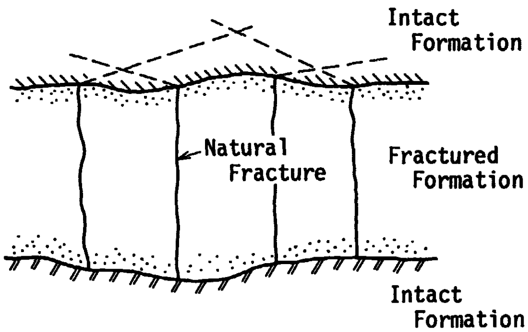

Figure 1. Fractured formation between intact formations.

up by the fracturing fluid. The other fractures remain being closed because of higher compressive stresses and pressure drop due to the flow resistance along the fluid paths. Along the closed fractures, the fracturing fluid flows through apertures which have been formed naturally by selfpropping caused by asperities on the fracture surfaces.
In this section, the growth process of a reservoir system of this kind during hydraulic fracturings is analyzed. The opened region in the reservoir system is modeled as a crack on an interface with infinitesimally small fracture toughness.

Figure 2 is the plane view of a reservoir system formed along natural fractures, where the fluid-filled region is hatched. The fractures are

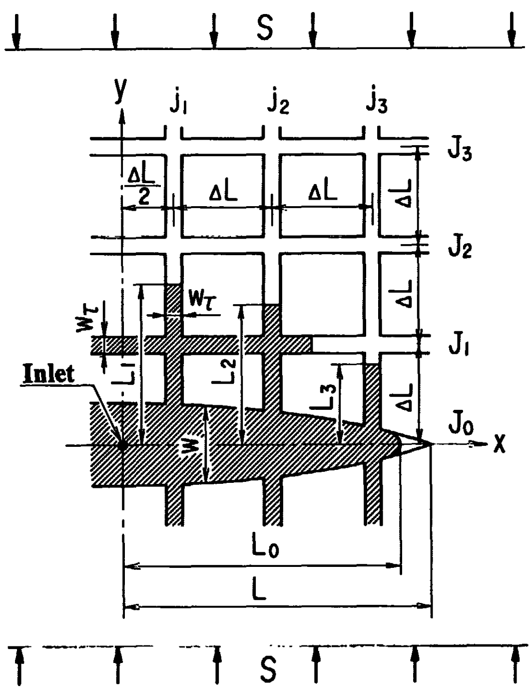

Figure 2. Plane view of reservoir system growing along natural fractures.

assumed to be on a regular rectangular grid with spacing ΔL. A Cartesian coordinate system (x, y) centered at the inlet is introduced. The fractures parallel to the x and y axes are denoted by J_i ($i = 0,1,2, \cdots$) and j_k ($k = 1,2,3, \cdots$) respectively, and the length of the fluid-filled region on j_k is denoted by L_k. The minimum compressive stress S of the tectonic stress is presumed to be acting normal to the fractures J_i. The fracture J_0 is opened up along the region $|x| < L$, where the fluid is filling the region $|x| < L_0$. The apertures of the opened fracture and the closed fractures are denoted by w and w_τ, where the aperture of the closed fractures is assumed to be independent of fluid pressure. The rock is under the condition of plane stress.

The volume flow rate q per unit thickness along J_0 is given by

$$q = \begin{cases} q_{in} - \displaystyle\int_0^x \frac{\partial w}{\partial t}\,dx & \text{for } 0 \leqq x < \dfrac{\Delta L}{2} \\ q_{in} - 2\displaystyle\sum_{i=1}^{m} q_i - \int_0^x \frac{\partial w}{\partial t}\,dx & \text{for } \dfrac{\Delta L}{2} \leqq x \leqq L_0 \end{cases} \qquad (1)$$

where m is the maximum integer less than $x/\Delta L$ and t is time. The half of the flow rate at the inlet and the rate of flow into the fracture j_i from the fracture J_0 are denoted by q_{in} and q_i ($i = 1,2,3, \ldots$), respectively.

The condition of global continuity of fluid flow in J_0 leads to

$$q_{in} - 2\sum_{i=1}^{n} q_i = \frac{\pi}{4}\left\{\frac{dL_0}{dt}\,w(L_0,t) + \int_0^{L_0} \frac{\partial w}{\partial t}\,dx\right\} \qquad (2)$$

where n is the maximum integer less than $L_0/\Delta L + 1/2$. According to the cubic law for the Newtonian flow in a narrow slit, the fluid pressure p in J_0 is given by

$$p = p_{in} - \int_0^x \frac{12\mu}{w^3}\,q\,dx \qquad (3)$$

where p_{in} is the pressure at the inlet and μ is the fluid viscosity. Equation (3) leads to

$$p_{in} = \int_0^{L_0} \frac{12\mu}{w^3}\,q\,dx \qquad (4)$$

since p (L_0, t) = 0. Similarly, the fluid pressure p_m at the point of intersection between the fractures J_0 and j_m can be obtained as follows:

$$p_m = p_{in} - \int_0^{\frac{2m-1}{2}\Delta L} \frac{12\mu}{w^3}\,q\,dx \qquad (5)$$

The flow pattern at an intersection point between two fractures (say J_k and j_m) can be classified into the three cases shown in fig. 3. In the case (a), the condition of continuity of the fluid flow and the equation of motion along the fracture j_m lead to

$$q_m = w_\tau \frac{dL_m}{dt}, \quad p_m = \frac{12\mu q_m}{w_\tau^3} L_m \tag{6}$$

Similarly, for the case (b)

$$q_m = 2w_\tau \frac{dL_m}{dt}, \quad p_m = \frac{12\mu q_m}{w_\tau^3} \frac{L_m+k\Delta L}{2} \tag{7}$$

For the case (c)

$$q_m = 3w_\tau \frac{dL_m}{dt}, \quad p_m = \frac{12\mu q_m}{w_\tau^3} \frac{L_m+2k\Delta L}{3} \tag{8}$$

In deriving equations (6)-(8), it is assumed that, after the fluid fills the flow path entirely between two neighboring grid points on the fracture J_k ($k = 1,2,3, \cdots$), the fluid does not flow between the two grid points. We analyzed also the case that allows the fluid to flow between such two grid points. The numerical results showed that the difference in the main reservoir size L between the two cases just stated became larger as w_τ. However, the difference is less than 10%, which could be allowable for the estimation of the reservoir size.

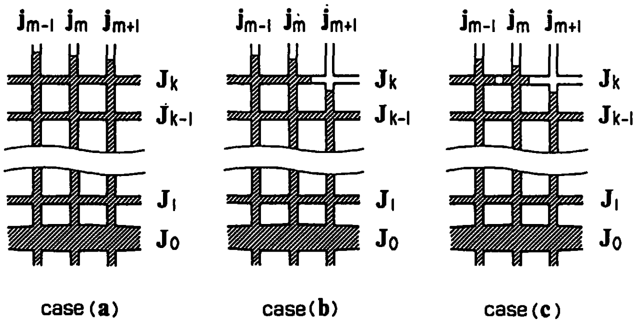

Figure 3. Flow patern around the point of intersection between J_k and j_m.

Now, let us analyze the elastic response of the rock. A statically equivalent pressure $\bar{p}$ is introduced for p in J_0, where $\bar{p}$ is the average value of p over the region $|x| \leqq L_0$, i.e.,

$$\bar{p} = \frac{1}{L_0}\int_0^{L_0} p \, dx \tag{9}$$

Then, w is approximated in the following form for $1-L/L_0 << 1$:

$$w = w_0\sqrt{1 - \frac{x^2}{L^2}} \tag{10}$$

The opened region of the fracture J_0 must be closed smoothly at its ends. This condition requires

$$\bar{p} = S + \frac{Gw_0}{2(1-\nu)L} \tag{11}$$

where G and ν are the shear modulus and the Poisson's ratio, respectively.

A set of ordinary differential equations involving first derivatives of L_i ($i = 1,2,3, \cdots$), L and w_0 with respect to time is obtained by substituting eqs. (1), (3), (4), (9) and (10) into eq. (11), eqs. (1), (6) and (10) into eq. (5) and eqs. (6) and (10) into eq. (2). It should be noted that, for the cases (b) and (c) (fig. 3), eqs. (7) and (8) must be used instead of eq. (6), respectively. The differential equations have been integrated numerically by the Runge-Kutta-Gill method.

The tectonic stress S is assumed to be

$$S = \alpha \rho_r g h \tag{12}$$

where α is the coefficient of the active rock pressure, ρ_r the density of the rock mass, g the acceleration due to the gravity, h the depth of the reservoir. The following values have been used:

$$G = 1.56 \times 10^4 \text{MPa},$$
$$\nu = 0.12,$$
$$\mu = 3.15 \times 10^{-4} \text{Pa·sec},$$
$$h = 4000\text{m},$$
$$\Delta L = 10\text{m},$$
$$\alpha = 0.5,$$
$$\rho_r = 2.5 \times 10^3 \text{kg/m}^3,$$
$$g = 9.8\text{m/sec}^2$$

The flow rate q_{in} is chosen to be 1.0×10^{-3} m³/sec·m with reference to the data of the massive hydraulic fracturings performed in the course of the Geothermal Project of Camborne School of Mines, UK. The height of the fractured formation is set to be 100m and the aperture w_τ is chosen to be 0 ~ 50μm. The flow resistance in such an aperture corresponds to that due to the permeability ranging from 0 to 2×10^{-10}m², which would be appropriate for the permeability of natural fractures (Kazemi, 1969; Preuss, 1983; Pulskamp, 1986).

The size L of the main reservoir is shown in fig. 4. It can be seen that the effect of fluid flow into natural fractures from the main reservoir is negligibly small if the aperture w_τ of the natural fractures is less than 10μm, which is equivalent to the permeability of 8.3×10^{-12}m². A typical example of the shape of the reservoir system is shown in fig. 5. The reservoir system can be approximated by an ellipse. The aspect ratio of the ellipse (L_1/L) is plotted with respect to time in fig. 6, where L_1 is defined in fig. 2. It can be seen that the aspect ratio increases in the early stage of fluid interjection and then levels off, i.e., the reservoir system grows up without changing its shape after some amount of fluid is injected.

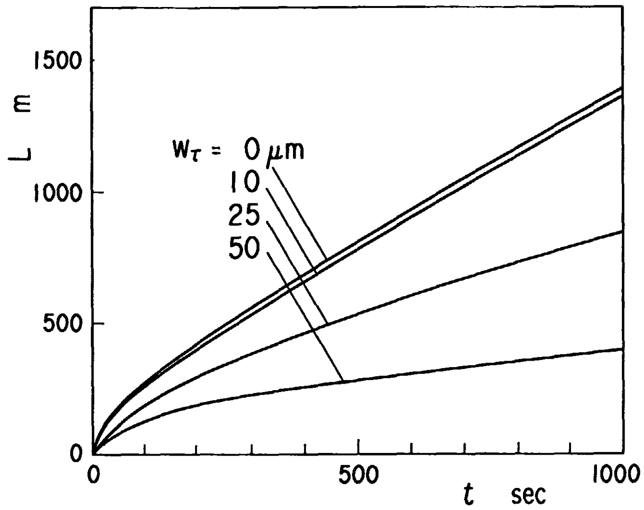

Figure 4. Variation of the main reservoir size with respect to time.

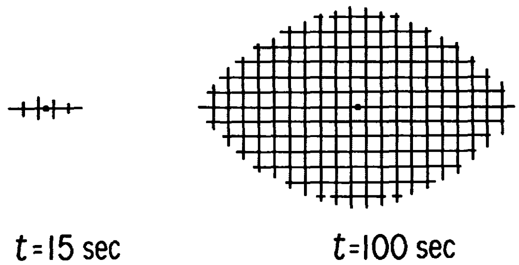

Figure 5. Typical examples of the shape of the reservoir system (w_T = 50μm).

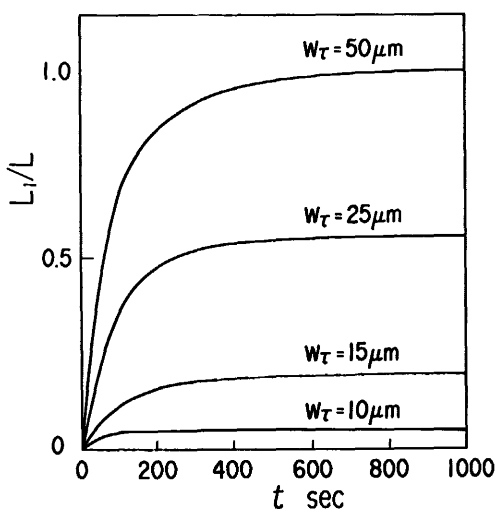

Figure 6. Variation of the reservoir aspect ratio with respect to time.

CIRCULATION OF FLUID

Let us provide two outlets at $x = \pm L_{out}$ to the reservoir system considered in the previous section (fig. 7), inject fluid from the inlet and recover it from the outlets. The fluid pressure and the volume flow rate at each outlet are denoted by p_{out} and q_{out}, respectively.

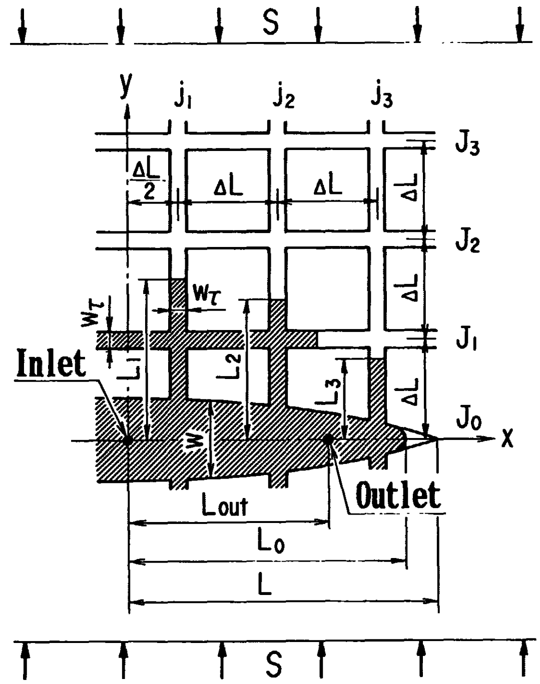

Figure 7. Reservoir system with the inlet and the outlets.

The volume flow rate q per unit thickness along J_0 are given by

$$q = \begin{cases} q_{in} - \int_0^x \frac{\partial w}{\partial t}dx & \text{for} \quad 0 \leqq x < \frac{\Delta L}{2} \\ q_{in} - 2\sum_{i=1}^{m} q_i - \int_0^x \frac{\partial w}{\partial t}dx & \text{for} \quad \frac{\Delta L}{2} \leqq x < L_{out} \\ q_{in} - q_{out} - 2\sum_{i=1}^{m} q_i - \int_0^x \frac{\partial w}{\partial t}dx & \\ & \text{for} \quad L_{out} \leqq x < L_0 \end{cases} \tag{13}$$

where m is the maximum integer less than $x/\Delta L+1/2$. The global continuity of fluid flow in J_0 requires

$$q_{in} - q_{out} - 2\sum_{i=1}^{n} q_i = \frac{\pi}{4}\left\{\frac{dL_0}{dt} w(L_0,t) + \int_0^{L_0} \frac{\partial w}{\partial t}dx\right\} \tag{14}$$

From eq. (3), the fluid pressure at the outlets is given by

$$p_{out} = p_{in} - \int_0^{L_{out}} \frac{12\mu}{w^3} q \, dx \qquad (15)$$

Equations (3)-(11) still hold. These equations and eqs. (13) and (14) can be reduced to a set of ordinally differential equations involving the first derivatives of L_i ($i = 1,2,3, \cdots$), L and w_0 with respect to time, following exactly the same procedure as that in the previous section. Equation (15) serves as the equation which determines q_{out} for given q_{in} and p_{out}.

In the numerical calculations, the distance between the outlets and the inlet and p_{out} are chosen to be 50m and 1.05S, respectively. Regarding G, ν, μ, h, ΔL, α, ρ_r, g and q_{in}, the same values as in the previous section have been used.

The rate of q_{out} to q_{in} is shown in fig. 8, where t_{out} is the time when the extraction of fluid starts through the outlets and is set to be 200sec. Just after the circulation starts, the fluid pressure in the reservoir system rapidly decreases because p_{out} is set to be lower than the pressure at the outlets before the circulation starts and, therefore, the aperture of the main flow path J_0 decreases. This makes q_{out} larger than q_{in} in the early stage of the circulation. It should be noted that more than 80% of the injected fluid is recovered even when the aperture of the natural fracture is 50μm. The permeability of such fractures is estimated to be $2 \times 10^{-10} m^2$ if the cubic law of the fluid flow through a narrow slit is adopted.

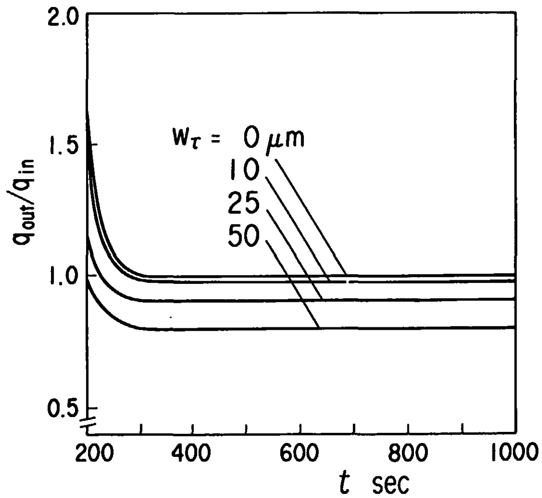

Figure 8. Rate of q_{out} to q_{in} against time.

Figure 9 shows the size L of the main reservoir. As in the previous section, the effect of fluid flow into the natural fractures from the main reservoir is negligibly small if the aperture w_T of the natural fracture is less than 10μm. It is also seen that the growth rate of the reservoir decreases drastically with time. This is due to the fact that the most amount of fluid injected through the inlet is recovered through the outlets as shown in fig. 8.

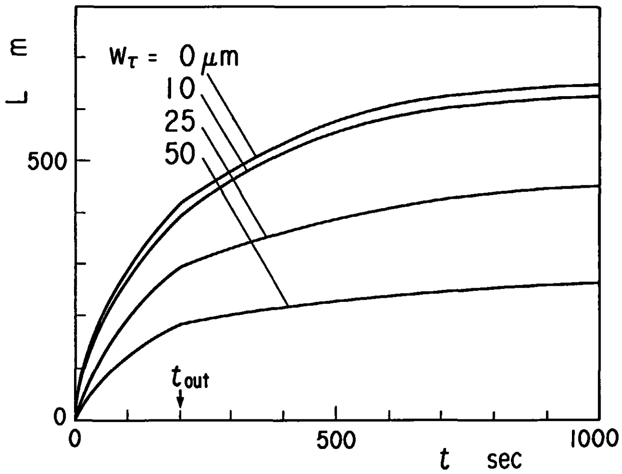

Figure 9. Variation of the main reservoir size with respect to time during fluid circulation.

The shape of the reservoir system is elliptical as in the case of the previous section, although the figures like fig. 5 are not presented here for brevity. The variation of the aspect ratio of the reservoir system with respect to time is shown in fig. 10. The aspect ratio has a tendency to level

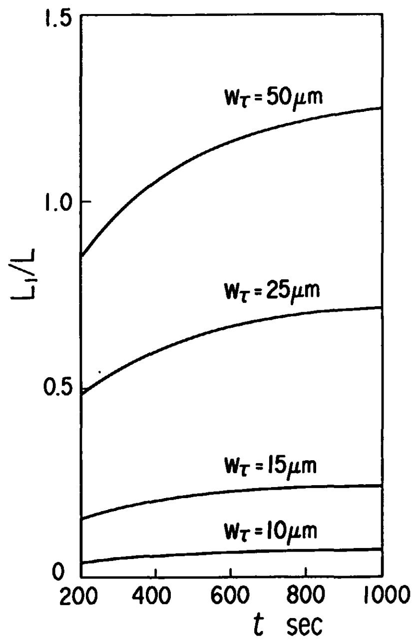

Figure 10. Variation of the reservoir aspect ratio with respect to time during fluid circulation.

off with time, i.e., the reservoir system grows up without changing its shape after its grows up to some extent.

CONCLUTION

Growth behavior of an artificially created reservoir system in a formation with a natural fracture network is analyzed for HDR geothermal heat extraction. The general conclusions that can be drawn from the present study are as follows:
(1) The artificial reservoir system in a formation with a fracture network grows up with an elliptical shape. The aspect ratio of the ellipse tends to level off after it grows up to some extent, i.e., the reservoir system does not change its shape.
(2) The growth rate of the reservoir system rapidly decreases with time after the circulation of fluid starts.
(3) The fluid loss during the circulation of fluid is fairly small and the most amount of the injected fluid is recovered: more than 80% of the injected fluid is recovered when the permeability of the natural fractures is less than $2 \times 10^{-10} m^2$.
(4) Thus, even when a natural fracture network exists in a formation, it would be possible to extract heat from such a formation by using an artificially created reservoir system.

ACKNOWLEDGEMENTS

The work presented here was supported by Ministry of Education, Science and Culture under Grant-in-Aid for Specially Promoted Research 58065002.

REFERENCES

Cundall, P. A., 1983, Development of Generalized 2-D and 3-D Distinct Element Programs for Modelling Jointed Rocks, US Army Engineers Waterways Experiment Station, Final Report.

Garnish, J. D., 1985, Hot Dry Rock — A European Perspective, Geoth. Resour. Coun. Trans., Int. V. associated with v. 9, p. 329-337.

Kazemi, H., 1969, Pressure Transient Analysis of Naturally Fractured Reservoirs with Uniform Fracture Distribution, Soc. Pet. Eng. J., v. 9, p. 451-462.

Murphy, H., 1982, Modelling Hydraulic Fracturing in Jointed Rock, Camborne School of Mines Geothermal Project Memo 13/04/01, Camborne School of Mines, Cornwall.

Pine, R. J. and Cundall, P. A., 1985, Application of the Fluid-Rock Interaction Program (FRIP) to the Modeling of Hot Dry Rock Geothermal Systems, Proc. Int. Symp. Fundamentals of Rock Joints, Centenk Pub., p. 293-302.

Preuss, K., 1983, Heat Transfer in Fractured Geothermal Reservoir with Boiling, Water Resour. Res., v. 191, p. 201-208.

Pulskamp, J. F., 1986, Experimental Tracer Response Curves for Fractured Cores, Geoth. Resour. Coun. Trans., v. 10, p. 395-398.

Takahashi, H. and Abé, H., 1988, Design Methodology of Artificial Crack-Like Reservoirs for HDR Geothermal Energy Extraction — An Overview of the Gamma Project in Japan, Energy-Sources Technology & Exhibition, ASME Publication, Geoth. Ener. Symp., p. 25-32.

Smith, M. C., et al., 1973, Induction Growth of Fractures in Hot Dry Rock, Geothermal Energy, P. Kruger and C. Otto, eds., Stanford Univ. Press, p. 251-268.

Whetten, J., et al., 1987, The US Hot Dry Rock Project, Geothermics, v. 16, p. 331-340.